View metadata, citation and similar papers at core.ac.uk
brought to you by CORE
provided by idUS. Depósito de Investigación Universidad de Sevilla

Transfer of Individual Micro- and Nanoparticles for High-Precision 3D Analysis Using 360° Electron Tomography

*Thomas Przybilla, Benjamin Apeleo Zubiri, Ana M. Beltrán, Benjamin Butz, Albert G. F. Machoke, Alexandra Inayat, Monica Distaso, Wolfgang Peukert, Wilhelm Schwieger, and Erdmann Spiecker**

A versatile approach is demonstrated, providing a general routine for an extensive and advanced 3D characterization of individually selected micro- and nanoparticles, enabling the combination of complementary and scale-bridging techniques. Quintessential to the method is the transfer of individual particles onto tailored tips using a conventional scanning electron microscope equipped with a suitable micromanipulator. The method enables a damage- and contamination-free preparation of freestanding particles. This is of significant importance for applications addressing the measurement of structural, physical, and chemical properties of specifically selected particles, such as 360° electron tomography, atom probe tomography, nano X-ray tomography, or optical near-field measurements. In this context, the method is demonstrated for 360° electron tomography of micro-/macroporous zeolite particles with sizes in the micrometer range and mesoporous alpha-hematite nanoparticles exhibiting sizes of 50–100 nm, including detailed pre- and post-characterization on the nanoscale.

1. Introduction

Particles with sizes in the nanometer to micrometer range are used in diverse fields of research and application such as catalysis,[1–3] drug delivery,[4,5] sensing,[6–9] optics,[10,11] electronics,[12,13] or optoelectronics.[14,15] As the particle design rises in complexity, a detailed and correlative characterization of their properties, for example, morphology, crystallographic structure, chemical composition, and physical properties, becomes indispensable in order to understand and prospectively design functionality.

Such investigations especially necessitate site-specific characterization techniques like atom probe tomography (APT), the broad spectrum of transmission electron microscopy (TEM) techniques, or single particle measurements of physical properties using, for example, near-field optical or spectroscopic techniques. Complementary to 2D imaging and analytical TEM techniques, electron tomography (ET) enables the 3D analysis of micro- and nanoparticles regarding their 3D morphology,[16–18] chemical properties (e.g., composition[19,20] or ionization states[21,22]), and physical properties (e.g., plasmonic eigenmodes[23]). In particular, 360° ET enables the investigation of freestanding samples without support and therefore avoids severe missing-wedge artifacts resulting from the limited tilt angular range in conventional ET.[24,25] However, 360° ET necessitates rod-shaped specimens with limited projected thickness to facilitate full rotation of the sample under similar imaging conditions. Concerning the preparation of individual nanoparticles, this sample geometry was realized in the past by cutting thin pillars out of embedded[26] or covered[27] nanoparticulate samples using focused ion beam (FIB) milling, or by dispersing particles in solution onto a suited tip.[28,29] However, these techniques bring along several drawbacks. In the first instance, they are rather statistical in nature and therefore do not allow for the selection of relevant particles out of the particle ensemble. Furthermore, there is usually the need for an embedding material or protective layer for FIB preparation. Such layers severely impair TEM image contrast with strong impact on the quality of the subsequent tomographic reconstruction. This is particularly detrimental for porous particles where undesired infiltration cannot

T. Przybilla, Dr. B. Apeleo Zubiri, Dr. A. M. Beltrán,[+] Dr. B. Butz, Prof. E. Spiecker
Center for Nanoanalysis and Electron Microscopy (CENEM) and Institute of Micro- and Nanostructure Research
Friedrich-Alexander-Universität Erlangen-Nürnberg
Cauerstraße 6, 91058 Erlangen, Germany
E-mail: erdmann.spiecker@fau.de

Dr. A. G. F. Machoke, Dr. A. Inayat, Prof. W. Schwieger
Institute of Chemical Reaction Engineering
Friedrich-Alexander-Universität Erlangen-Nürnberg
Egerlandstrasse 3, 91058 Erlangen, Germany

Dr. M. Distaso, Prof. W. Peukert
Institute of Particle Technology
Friedrich-Alexander-Universität Erlangen-Nürnberg
Cauerstraße 4, 91058 Erlangen, Germany

Dr. M. Distaso, Prof. W. Peukert, Prof. W. Schwieger, Prof. E. Spiecker
Center of Functional Particle Systems
Friedrich-Alexander-Universität Erlangen-Nürnberg
Haberstraße 9a, 91058 Erlangen, Germany

[+]Present address: Departamento de Ingeniería y Ciencia de los Materiales, Escuela Técnica Superior de Ingeniería, Universidad de Sevilla, Camino de los Descubrimientos, s/n, Isla de la Cartuja, 41092 Sevilla, Spain

DOI: 10.1002/smtd.201700276

© 2017 WILEY-VCH Verlag GmbH & Co. KGaA, Weinheim

be avoided and may even change the fragile inner structure of the particle. However, the most fundamental drawback of a protective layer or embedding material is that the particle under investigation is no longer in its original (surface) state principally impeding direct correlation of quantitative 3D information (from 360° ET) with single particle measurements of physical properties like plasmonic resonances. Therefore, a robust preparation method is required, which enables the transfer of an individually selected particle in its original (uncovered) state onto a tip, so that the particle is accessible from all sides.

Although micromanipulation techniques in a modern scanning electron microscopy (SEM) instrument offer great potential for a robust, repeatable, and simple transfer of single, individual micro- and nanoparticles, no standardized routine has been established so far. In a recent study by Felfer et al., a microgripper/piezo substage combination (Kleindiek lift-out shuttle) was utilized to in situ transfer µm-sized nanoparticle agglomerates in the SEM machine onto tips for APT.[30] The resulting agglomerates on the tip were subsequently thinned with the FIB instrument to match the respective sample geometry. However, adhesion effects as well as the bulky geometry of the microgripper complicate a reliable and precise transfer of single nanoparticles. Another approach involves micromanipulation, which is based on atomic force microscopy (AFM), to handle nm-sized objects.[31,32] However, AFM manipulation processes cannot be observed in real time and are typically more complicated than a SEM in situ transfer. New concepts utilize an AFM inside a SEM instrument to manipulate nano-objects,[33,34] which allow precise adjustment, control, and flexibility as well as in situ real-time observation. However, these approaches rely on highly specialized equipment and are therefore not suited for widespread use.

In this work, a procedure is described which enables in situ transfer of a single, individually selected particle from a suitable substrate onto a tailored tip, as it is commonly used for 360° ET or APT. The procedure only necessitates a conventional SEM (or dual-beam SEM/FIB) instrument equipped with a suitable micromanipulator and can therefore be implemented in any modern laboratory. A flexible sample mounting geometry is employed, which allows for fast screening of a statistically relevant number of particles as well as detailed pre-characterization of the selected particle using SEM and TEM.

The proposed method enables to obtain freestanding particles without preparation artifacts and modification of the particle surface, as no FIB milling[35] is involved and therefore no protective layer is needed. This is not only highly advantageous for 360° ET and complementary characterization techniques like APT,[30] but furthermore offers the unique possibility to measure physical properties[36] of the selected particle in the same geometry by applying, for example, optical near-field microscopy[23,37,38] or other sub-µm probes. After the nondestructive particle characterization, further in situ testing, FIB tomography, or FIB lamella preparation for high-resolution TEM (HRTEM) analyses can still be applied. In particular, the obtained 3D information can be directly combined with mechanical data from subsequent (in situ) mechanical testing. Therefore, the method is a complement for the existing sample preparation method to disperse particles in solution on a silicon wedge for compression of particles by in situ TEM.[39,40]

2. Results

The particle transfer method is schematically depicted in **Figure 1**. The workflow comprises particle preparation, particle selection and pre-characterization, in situ "stamping transfer," 3D analysis by 360° ET, and optional post-characterization.

In the first step, the particles are sparsely dispersed onto a suitable support grid typically used for TEM studies. The grid is mounted into the SEM and fixed at the front end of a micromanipulator equipped with a clamp. A dedicated tomography tip is vertically mounted onto the stage of the microscope below the TEM grid as it is drawn in **Figure 2**.

Different SEM imaging modes are employed for screening the particle ensemble and selecting a suitable particle located at the bottom surface of the support film. Alternatively, particle selection and pre-characterization can be carried out in the TEM prior to insertion of the grid in the SEM (Figure 1). The particle is subsequently picked up with the tomography tip from

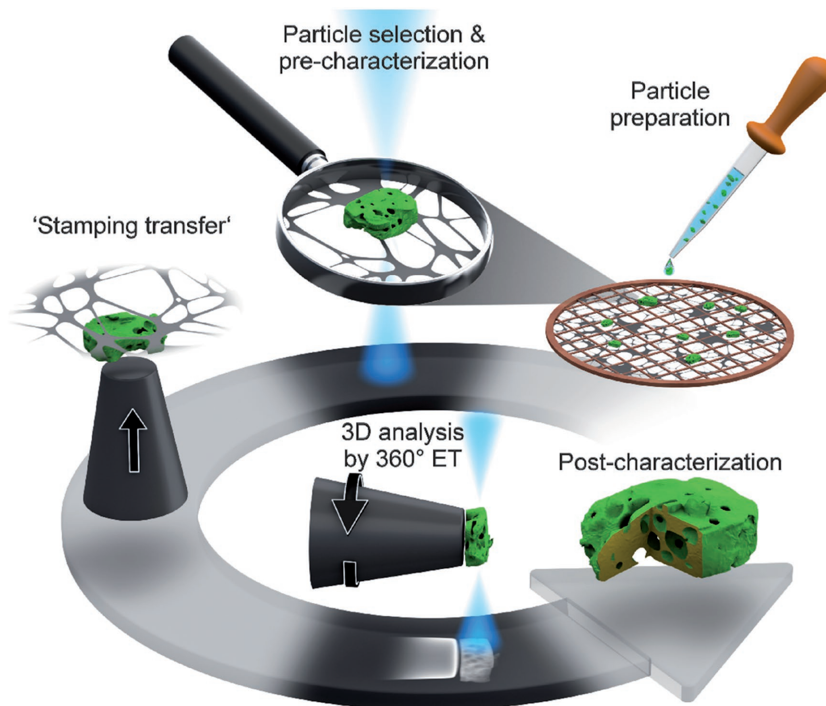

Figure 1. Schematic flowchart illustrating preparation, pre-characterization, and in situ "stamping transfer" technique for 360° ET of individually selected micro-/nanoparticles enabling high-precision 3D analysis. The depicted particle is a visualization of the tomographic reconstruction of the porous particle shown in Figures 3 and 4. The "stamping transfer" technique is not restricted to porous particles but is applicable to almost any kind of particle.

© 2017 WILEY-VCH Verlag GmbH & Co. KGaA, Weinheim

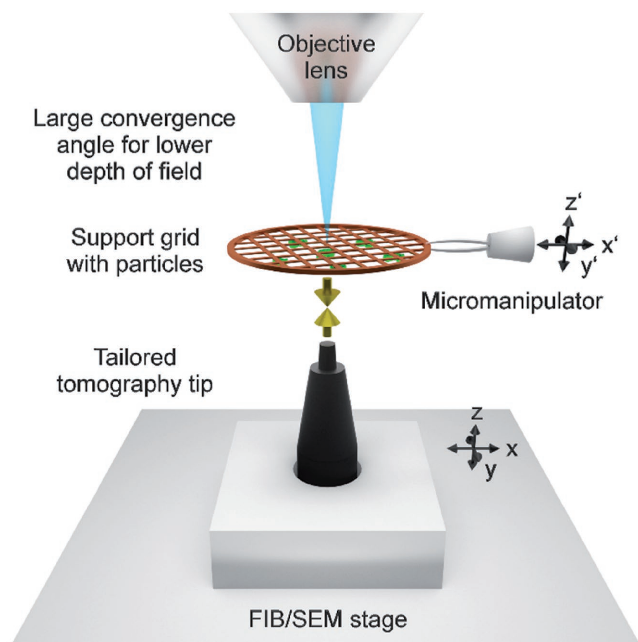

Figure 2. Sketch of the experimental setup for the "stamping transfer" procedure in the SEM instrument: the support grid with particles connected to a micromanipulator with a clamp and the microscope stage with the tailored tomography tip are approached to attach one selected particle to the plateau of the tip. Improved height control is achieved by monitoring the procedure with an electron beam of large convergence angle (reduced depth of field). For more details, please refer to the Supporting Information.

the support film by direct "stamping" (Figures 1 and 2). Details of this procedure, which involves (i) carefully approaching the particle with the tip (or vice versa), (ii) establishing an intimate contact, and (iii) detaching the particle from the support film, are described in the Supporting Information. If a FIB-SEM is available, it is recommended to pre-shape the tip to create a plateau slightly larger than the particle (**Figure 3**d and 5d, and Figure S1, Supporting Information). After successful particle transfer, the tomography tip with the particle positioned on top is transferred to the TEM, where a tilt series with full tilt-angle range is acquired. The 3D reconstruction of the tilt series finally allows a high-precision 3D analysis of the particle without neither preparation nor missing-wedge artifacts. Therefore, the digitally reconstructed volume can directly be used for quantitative 3D analyses, modeling, and simulations. Since 360° ET is a nondestructive method, the sample can afterward be employed for a detailed post-characterization, for further in situ experiments or for measurements of single particle physical properties. In the following, the applicability of the "stamping transfer" method is demonstrated for particles in the micrometer range (Figure 3 and **Figure 4**) as well as for nanoparticles with sizes in the range of 50–100 nm (**Figure 5** and **6**).

The first example comprises the 3D investigation of micro/macroporous MFI-type zeolite particles prepared by a recently developed method based on steam-assisted crystallization of impregnated mesoporous silica particles.[2] The particles show rather uniform morphology with typical dimensions of $4 \times 2.5 \times 3\ \mu m^3$ and incorporate intracrystalline macropores with diameters ranging from 250 to 500 nm (Figure 3a). In the first step, the particles are dispersed on a TEM grid with

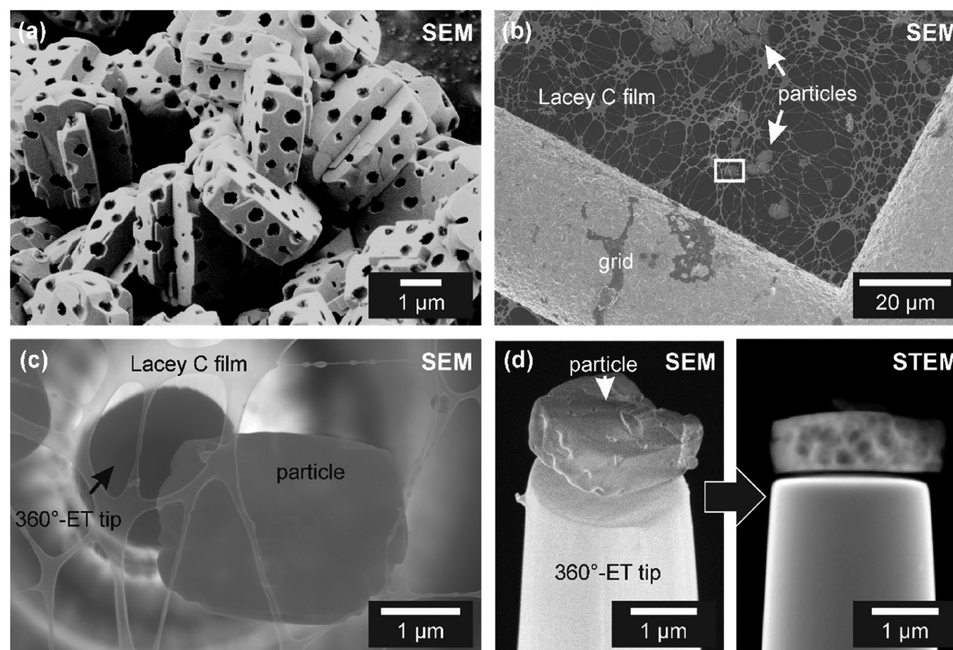

Figure 3. Experimental realization of the particle "stamping transfer" technique for µm-sized zeolite particles in a FIB/SEM instrument. a) SEM image of a particle ensemble, b) top view of the selection of an individual particle lying on a Lacey carbon support film, and c) the approaching tomography tip toward the particle from below for subsequent particle transfer. Please note that the tip was coated prior to the "stamping transfer" with SEM-compatible glue for adhesion enhancement (see the Supporting Information for more details). Contrast changes of the Lacey carbon film and the particle in (c) are due to an increased electron transparency caused by usage of a higher e-beam energy, which facilitates to approach the tip. d) As-transferred particle in the FIB/SEM machine (perspective view) and the TEM instrument (side view, STEM mode).

 © 2017 WILEY-VCH Verlag GmbH & Co. KGaA, Weinheim

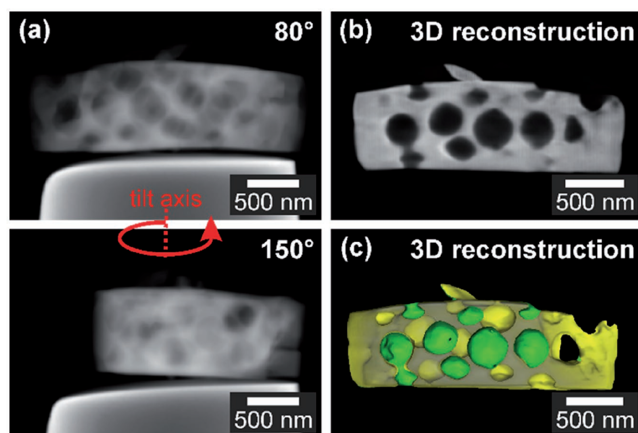

Figure 4. 360° ET of the transferred porous zeolite particle from Figure 3. a) Two representative STEM images from the full tilt-angle range series at different tilt angles (see Movie S1, Supporting Information). b) Slice through 3D reconstruction and c) respective surface rendering (surface facing toward the pore space in green and the particle interior in yellow) sliced at the same position as in (b) (see Movie S2, Supporting Information).

Lacey C film (Figure 3b) allowing for screening of the particle ensemble followed by particle selection and pre-characterization using the various modes of SEM and TEM. Results of a detailed TEM investigation including single-particle electron diffraction and high-resolution TEM imaging are summarized in Figure S2 (Supporting Information) confirming that the particles are single-crystalline with MFI crystal structure. They exhibit pronounced facets and are typically lying on their largest facet on the support film. For applications as catalytic material, the 3D investigation of their pore structure is of high importance, for example, to analyze the interconnectivity and accessibility of the embedded macropore system.[41]

To perform the particle "stamping transfer" according to the scheme shown in Figure 1, one characteristic particle with interconnected macropores was selected (Figure 3b) and transferred onto a tomography tip (Figure 3c,d). Prior to that, the tip diameter was adapted to match the particle dimensions and the tip plateau was flattened by FIB milling. Furthermore, the adhesion forces between the tomography tip (brass) and the zeolite particle were increased using SEM-compatible glue prior to the particle transfer (Figure S1, Supporting Information). Figure 3d shows the as-transferred, freestanding particle in the SEM and TEM instruments.

It becomes evident that the particle is exactly located on the uppermost part of the tip. No shadowing effects of the tomography tip occur during acquisition of the full tilt-angle range series in the TEM (Figure 4a and Movie S1, Supporting Information). This allows for a high-quality 3D reconstruction (Figure 4b,c and Movie S2, Supporting Information) and subsequent quantitative analysis, for example, by determining the pore size distribution of the particle (Figure S4, Supporting Information). Figure S3 (Supporting Information) demonstrates the high improvement of the reconstruction quality of 360° ET in comparison to conventional ET, where the limited tilt-angle range due to shadowing effects of the sample and the sample holder induces missing-wedge artifacts to the 3D reconstruction.

After 360° ET investigation, the particle can be used for further characterization and experiments. Figure S2c (Supporting Information) exemplarily shows a bright field TEM (BF-TEM) image and a HRTEM image of a thin lamella which was cut out of another porous zeolite particle using the FIB lift-out

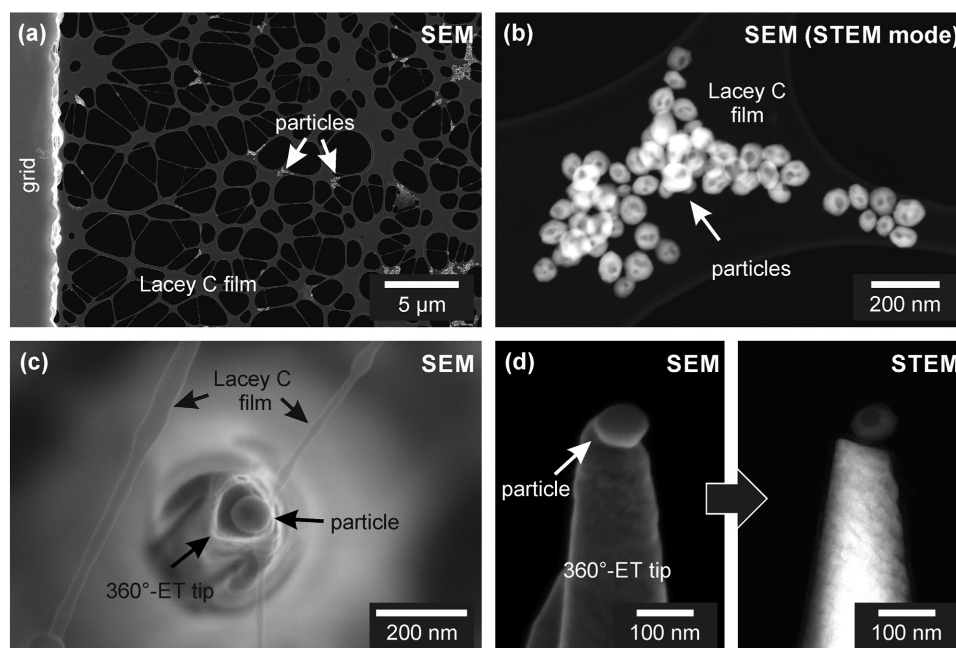

Figure 5. Experimental realization of the particle "stamping transfer" technique for hematite nanoparticles in the FIB/SEM instrument. a) Overview and b) pre-characterization of different particles with enclosed porosity dispersed on a Lacey carbon support film in STEM mode and c) approaching tomography tip toward the particle from below for subsequent particle transfer (all top views). d) As-transferred particle in the FIB/SEM instrument (perspective view) and TEM machine (side view, STEM mode).

© 2017 WILEY-VCH Verlag GmbH & Co. KGaA, Weinheim

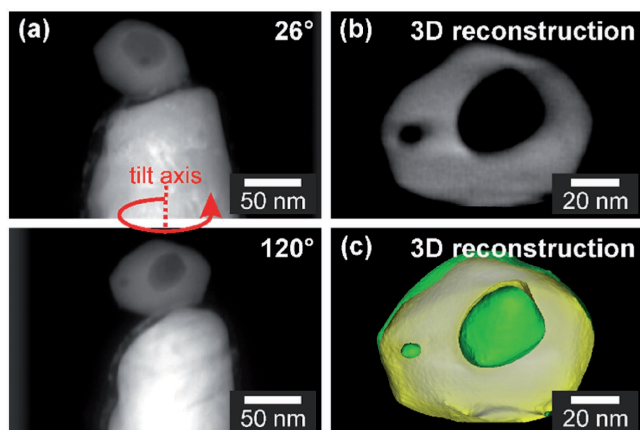

Figure 6. 360° ET of the transferred mesoporous hematite particle from Figure 5. a) Two representative STEM images from the full tilt-angle range series at different tilt angles (see Movie S3, Supporting Information). b) Slice through 3D reconstruction and c) respective surface rendering (surface facing toward the pore space in green and the particle interior in yellow) sliced at the same position as in (b) (see Movie S4, Supporting Information).

technique. This enables to simultaneously access the direct interface as well as the interconnection between the macro- and microporous domains of the MFI-type zeolite particle.

The second example demonstrates the feasibility of the transfer method for much smaller particles in the nanometer range. Different mesoporous alpha-hematite nanoparticles[29,42] with sizes of 50–100 nm were pre-characterized regarding their porosity (Figure 5a,b). The 3D investigation of their inner pore structure is of crucial importance for potential applications as pigments, catalyst support, or optoelectronics. A specific and representative particle was identified and transferred to the tip using the "stamping transfer" method (Figure 5c,d). The diameter of the tomography tip was tailored to match the particle size using FIB milling prior to the transfer procedure. In this case, adhesion forces between the hematite particle and the brass tip were sufficiently high, so that the particle directly stuck to the tip plateau and no SEM-compatible glue was required. The single nanoparticle remained stable and did not change its position on the tip plateau neither in the FIB/SEM instrument (Figure 5d) nor during tilt-series acquisition in the TEM (Figures 5d and 6a), which is of crucial importance for a precise reconstruction. Figure 6a shows two images from the full tilt-angle range series (also refer to Movie S3, Supporting Information), which were used for 3D reconstruction of the particle with its enclosed porosity (Figure 6b,c and Movie S4, Supporting Information). The hematite particle lies on the plateau of the tomography tip and experiences almost no shadowing of the tip during tilting. The high quality of the tomogram without missing-wedge artifacts allows for quantitative evaluation of the pore space (Figure S5, Supporting Information).

It should be noticed here that the undermost part of the particle close to the slightly inclined surface of the tip gets covered under certain angles during tilt-series acquisition (Figure 6a, and Movie S3, Supporting Information). This circumstance leads to an increased projected thickness in the lower region of the particle and therefore affects the reconstruction quality in that part. Since the employed tomography tips are typically crystalline, the reconstruction quality is slightly deteriorated due to possible contrast fluctuations, for example, residual diffraction contrast in STEM imaging mode, in the regions of the inclined surface. This influence can be avoided by depositing amorphous material, for example, carbon, onto the tomography tip before particle transfer. Completely flat tip plateaus will avoid both mentioned effects. This can be realized via FIB preparation by correcting the intensity tail of the ion beam profile by over-tilting the sample in a predefined angle instead of milling perpendicular to the tip axis.[43]

3. Discussion

The "stamping transfer" method, which is demonstrated in this work for particles in the micrometer (Figures 3 and 4) and sub-100 nm (Figures 5 and 6) range, has a number of advantages: first and foremost, it enables the flexible and reliable transfer of a single, individually selected particle after careful selection out of a large particle ensemble. The time-consuming 3D analysis can therefore be restricted to a few representative particles or to particles with special features of particular interest. Moreover, the method enables correlative 2D and 3D studies of one and the same particle by combining measurements on the grid and on the tip, respectively. From a practical point of view there are further advantageous features of the technique that should be mentioned. Since no highly specialized equipment is employed the technique can be implemented in any modern laboratory. Common support grids (Lacey, holey carbon, etc.) are used which are easily accessible and fit into standard TEM holders. The carbon support films turned out to be well suited since the low bending stiffness impedes mechanical alteration of the particle during transfer. In case of insufficient adhesion (between tip and particle) impeding the transfer of larger particles a special SEM-compatible glue can be used to assist the particle transfer as demonstrated in the first application example (cf. Figure 3 and Figure S1, Supporting Information). Finally, already dispersed and pre-investigated particle ensembles on suited TEM grids can be screened and utilized for 360° ET, even if the powder/solution is not available any more.

Next, we want to address potential improvements to the transfer method as a van der Waals (vdW) force actuated operation (without the utilization of SEM-compatible glue) referring to basic material interactions (please refer to the Supporting Information for a more detailed discussion). In short, the strength of van der Waals adhesion is determined by the Hamaker constants of grid and tip material. The adhesion force can further be tailored by adjusting the surface roughness. A higher surface roughness leads to a lower Van der Waals force. Relating to this, the "stamping transfer" method can be improved in terms of flexibility and reliability (without the use of adhesive interlayers) by selecting different materials and/or modifying the surface of either the grid and/or the tip. These modifications can be done by, for example, thin-film coating techniques,[44] plasma activation,[45] or wet chemical treatment.[46] To strengthen the adhesion between particle and tip, the tip can be coated with a material featuring a high Hamaker constant while ensuring a low surface roughness. Furthermore,

© 2017 WILEY-VCH Verlag GmbH & Co. KGaA, Weinheim

the tip can be functionalized, for instance, with a material that is polar, hydrophilic, or hydrophobic, depending on the studied particle system. Vice versa the grid can be coated with a material of low Hamaker constant and a high surface roughness to lower adhesion forces. Furthermore, the Lacey grid can be weakened by plasma cleaning, thus reducing the contact area by decreasing the number and diameter of carbon threads. Regarding these options adhesion forces can be balanced to cause the particle to adhere to the tip upon the slightest contact. As a practical example, the grid could be coated with a thin Al layer by standard physical vapor deposition techniques, choosing deposition parameters which lead to a high surface roughness, while using Cu as a tip material, ensuring a low surface roughness. A different approach could involve poly(tetrafluorethylene) (PTFE) as a grid coating due to its very low Hamaker constant ($H_{PTFE} = 3.8 \times 10^{-20}$ J).[47] As an outlook the method could be further modified using electrostatic forces by applying an electric potential between grid and tip to in situ transfer particles without direct contact.[48]

As demonstrated by the two applications the technique enables precise positioning of the chosen particle on the uppermost top plateau of the pre-shaped tomography tip. Concerning the accessible particle size the presented "stamping transfer" method is in principle only restricted by the resolution of the SEM instrument requiring the capacity to simultaneously recognize and observe the particle and tip during the transfer procedure. Presumably, particles ranging down to a size of about 10 nm can still be transferred using this technique. Therefore, the method is expected to be applicable to diverse types of particles with sizes ranging from about 10 nm to few 10 µm. This broad range covers all particles with dimensions, which typically impede a facile particle transfer using a conventional light microscope, for example, in combination with an external micromanipulator. For sufficiently small particles, the transfer technique potentially enables extraction of 3D information on the atomic scale. Several approaches to gather 3D information at atomic resolution by applying different TEM techniques are reported in literature, for example, by using high-resolution STEM images from few specific crystallographic directions[49,50] (discrete tomography), by conventional STEM tomography with special projection alignment and tomographic reconstruction,[51] by combining electron diffraction and conventional TEM imaging,[52] or even based on a single HRTEM image.[53,54] However, the combination of one of these techniques and 360° ET has not been reported yet. The in situ "stamping transfer" method paves the way for such combined 3D atomic scale studies on individually selected nanoparticles.

Apart from 360° ET the well-defined particle-on-tip geometry obtained with the method is also well suited for other fields of application. For instance, single particle measurements of physical properties,[36] like plasmonic modes[23] or other size-dependent optical properties can be carried out in this geometry using either optical near-field[37,38] or confocal microscopy techniques (including single particle Raman and photoluminescence (PL) spectroscopy[55,56]). Moreover, the geometry is perfectly suited for complementary characterization techniques like atom probe tomography.[30] Most importantly, such measurements can be directly correlated with the detailed 3D particle morphology obtained from nondestructive 360° ET.

4. Conclusion

In summary, we presented a new, versatile approach to in situ transfer individual micro- or nanoparticles, selected out of a large particle ensemble, onto tailored tips for high-precision 3D analysis using 360° ET. The method can be implemented on any modern SEM instrument and enables damage- as well as contamination-free preparation of particles in a broad size range. The obtained particle-on-tip geometry provides a general platform for correlative studies of 3D morphology and physical properties of individual nanoparticles.

Supporting Information

Supporting Information is available from the Wiley Online Library or from the author.

Acknowledgements

T.P. and B.A.Z. contributed equally to this work. E.S. and B.B. designed the studies. T.P. realized the FIB preparation technique, and B.A.Z. and A.M.B. performed the electron tomography investigations. M.D. and W.P. provided the hematite samples. A.G.F.M., A.I., and W.S. provided the zeolite samples. T.P., B.A.Z., B.B., and E.S. wrote the manuscript. All authors discussed the results and commented on the manuscript. The authors gratefully acknowledge the financial support of the "Deutsche Forschungsgemeinschaft" (DFG) within the framework of the SPP 1570 (project DFG SP 648/4-3 "3D analysis of complex pore structures using ET and high-resolution TEM") and the research training group GRK 1896 ("In situ Microscopy with Electrons, X-rays and Scanning Probes") as well as through the Cluster of Excellence "Engineering of Advanced Materials" at the Friedrich-Alexander-Universität Erlangen-Nürnberg (Germany). Christel Dieker is acknowledged for FIB preparation of the cross-sectional sample from the macroporous zeolite particle. The authors thank Julian Loscher for helping with the design and creation of Figure 1.

Conflict of Interest

The authors declare no conflict of interest.

Keywords

360° electron tomography, dual-beam SEM/FIB, micromanipulation, pick and place, sample preparation

Received: August 9, 2017
Revised: September 19, 2017
Published online: December 4, 2017

[1] L. Gan, M. Heggen, R. O'Malley, B. Theobald, P. Strasser, *Nano Lett.* **2013**, *13*, 1131.
[2] A. G. Machoke, A. M. Beltrán, A. Inayat, B. Winter, T. Weissenberger, N. Kruse, R. Güttel, E. Spiecker, W. Schwieger, *Adv. Mater.* **2015**, *27*, 1066.
[3] Z. Fan, H. Zhang, *Acc. Chem. Res.* **2016**, *49*, 2841.

© 2017 WILEY-VCH Verlag GmbH & Co. KGaA, Weinheim

[4] I. I. Slowing, B. G. Trewyn, S. Giri, V. S. Y. Lin, *Adv. Funct. Mater.* **2007**, *17*, 1225.
[5] K. Ulbrich, K. Hola, V. Subr, A. Bakandritsos, J. Tucek, R. Zboril, *Chem. Rev.* **2016**, *116*, 5338.
[6] K. Lee, M. A. El-sayed, *J. Phys. Chem. B* **2006**, *110*, 19220.
[7] B. H. McNaughton, R. R. Agayan, J. X. Wang, R. Kopelman, *Sens. Actuators, B* **2007**, *121*, 330.
[8] J. N. Anker, W. P. Hall, O. Lyandres, N. C. Shah, J. Zhao, R. P. Van Duyne, *Nat. Mater.* **2008**, *7*, 442.
[9] M. Sriram, K. Zong, S. R. C. Vivekchand, J. J. Gooding, *Sensors* **2015**, *15*, 25774.
[10] K. Liu, Y. Bai, L. Zhang, Z. Yang, Q. Fan, H. Zheng, Y. Yin, C. Gao, *Nano Lett.* **2016**, *16*, 3675.
[11] D. Segets, J. M. Lucas, R. N. K. Taylor, M. Scheele, H. Zheng, A. P. Alivisatos, W. Peukert, *ACS Nano* **2012**, *6*, 9021.
[12] C. K. Kim, G.-J. Lee, M. K. Lee, C. K. Rhee, *Powder Technol.* **2014**, *263*, 1.
[13] J.-H. Choi, H. Wang, S. J. Oh, T. Paik, P. S. Jo, J. Sung, X. Ye, T. Zhao, B. T. Diroll, C. B. Murray, C. R. Kagan, *Science* **2016**, *352*, 205.
[14] J. Schornbaum, B. Winter, S. P. Schießl, F. Gannott, G. Katsukis, D. M. Guldi, E. Spiecker, J. Zaumseil, *Adv. Funct. Mater.* **2014**, *24*, 5798.
[15] L. De Sio, T. Placido, R. Comparelli, M. L. Curri, M. Striccoli, N. Tabiryan, T. J. Bunning, *Prog. Quantum Electron.* **2015**, *41*, 23.
[16] H. B. Zhang, A. Takaoka, K. Miyauchi, *Rev. Sci. Instrum.* **1998**, *69*, 4008.
[17] E. Biermans, L. Molina, K. J. Batenburg, S. Bals, G. Van Tendeloo, *Nano Lett.* **2010**, *10*, 5014.
[18] N. Kawase, M. Kato, H. Nishioka, H. Jinnai, *Ultramicroscopy* **2007**, *107*, 8.
[19] T. J. A. Slater, E. A. Lewis, S. J. Haigh, *J. Vis. Exp.* **2016**, *113*, https://doi.org/10.3791/52815.
[20] P. Rueda-Fonseca, E. Robin, E. Bellet-Amalric, M. Lopez-Haro, M. Den Hertog, Y. Genuist, R. Andre, A. Artioli, S. Tatarenko, D. Ferrand, J. Cibert, *Nano Lett.* **2016**, *16*, 1637.
[21] P. Torruella, R. Arenal, F. de la Peña, Z. Saghi, L. Yedra, A. Eljarrat, L. López-Conesa, M. Estrader, A. López-Ortega, G. Salazar-Alvarez, J. Nogués, C. Ducati, P. A. Midgley, F. Peiró, S. Estradé, *Nano Lett.* **2016**, *16*, 5068.
[22] B. Goris, S. Turner, S. Bals, G. Van Tendeloo, *ACS Nano* **2014**, *8*, 10878.
[23] O. Nicoletti, F. de la Peña, R. K. Leary, D. J. Holland, C. Ducati, P. A. Midgley, *Nature* **2013**, *502*, 80.
[24] P. A. Midgley, R. E. Dunin-Borkowski, *Nat. Mater.* **2009**, *8*, 271.
[25] V. Novák, E. Ortel, B. Winter, B. Butz, B. Paul, P. Ko í, M. Marek, E. Spiecker, R. Kraehnert, *Chem. Eng. J.* **2014**, *248*, 49.
[26] X. Y. Wang, R. Lockwood, M. Malac, H. Furukawa, P. Li, A. Meldrum, *Ultramicroscopy* **2012**, *113*, 96.
[27] M. Hayashida, M. Malac, M. Bergen, P. Li, *Ultramicroscopy* **2014**, *144*, 50.
[28] K. Jarausch, D. N. Leonard, *J. Electron Microsc.* **2009**, *58*, 175.
[29] M. Distaso, B. Apeleo Zubiri, A. Mohtasebi, A. Inayat, M. Dudák, P. Koci, B. Butz, R. Klupp Taylor, W. Schwieger, E. Spiecker, W. Peukert, *Microporous Mesoporous Mater.* **2017**, *246*, 207.
[30] P. Felfer, T. Li, K. Eder, H. Galinski, A. Magyar, D. Bell, G. D. W. Smith, N. Kruse, S. P. Ringer, J. M. Cairney, *Ultramicroscopy* **2015**, *159*, 413.
[31] H. Xie, D. S. Haliyo, S. Régnier, *Nanotechnology* **2009**, *20*, 215301.
[32] B. Mokaberi, J. Yun, M. Wang, A. A. G. Requicha, in *IEEE Int. Conf. on Robotics and Automation*, IEEE, Piscataway, NJ, USA **2007**, p. 1406.
[33] M. Bartenwerfer, S. Fatikow, R. Tunnell, U. Mick, C. Stolle, C. Diederichs, D. Jasper, V. Eichhorn, in *IEEE Int. Conf. on Mechantronics and Automation*, IEEE, Piscataway, NJ, USA **2011**, p. 171.
[34] P. Banzer, P. Woźniak, U. Mick, I. De Leon, R. W. Boyd, *Nat. Commun.* **2016**, *7*, 13117; https://doi.org/10.1038/ncomms13117.
[35] J. Mayer, L. A. Giannuzzi, T. Kamino, J. Michael, *MRS Bull.* **2007**, *32*, 400.
[36] P. Banzer, U. Peschel, S. Quabis, G. Leuchs, *Opt. Express* **2010**, *18*, 10905.
[37] M. Fleischer, A. Weber-Bargioni, M. V. P. Altoe, A. M. Schwartzberg, P. J. Schuck, S. Cabrini, D. P. Kern, *ACS Nano* **2011**, *5*, 2570.
[38] M. Barth, S. Schietinger, T. Schröder, N. Nüsse, B. Löchel, T. Aichele, O. Benson, *J. Lumin.* **2010**, *130*, 1628.
[39] Z. W. Shan, G. Adesso, A. Cabot, M. P. Sherburne, S. A. S. Asif, O. L. Warren, D. C. Chrzan, A. M. Minor, A. P. Alivisatos, *Nat. Mater.* **2008**, *7*, 947.
[40] K. Zheng, C. Wang, Y.-Q. Cheng, Y. Yue, X. Han, Z. Zhang, Z. Shan, S. X. Mao, M. Ye, Y. Yin, E. Ma, *Nat. Commun.* **2010**, *1*, 24; https://doi.org/10.1038/ncomms1021.
[41] W. Schwieger, A. G. Machoke, T. Weissenberger, A. Inayat, T. Selvam, M. Klumpp, A. Inayat, *Chem. Soc. Rev.* **2016**, *45*, 3353.
[42] M. Distaso, O. Zhuromskyy, B. Seemann, P. Lukas, M. Ma, E. Encina, R. Klupp, R. Müller, G. Leugering, E. Spiecker, U. Peschel, W. Peukert, *J. Quant. Spectrosc. Radiat. Transfer* **2017**, *189*, 369.
[43] B. I. Prenitzer, L. A. Giannuzzi, K. Newman, S. R. Brown, R. B. Irwin, F. A. Stevie, T. L. Shofner, *Metall. Mater. Trans. A* **1998**, *29*, 2399.
[44] S. Matope, A. F. Van der Merwe, Y. I. Rabinovich, *South African J. Ind. Eng.* **2013**, *24*, 69.
[45] D. Hegemann, H. Brunner, C. Oehr, *Nucl. Instrum. Methods Phys. Res., Sect. B* **2003**, *208*, 281.
[46] A. Cammarano, G. De Luca, E. Amendola, *Cent. Eur. J. Chem.* **2013**, *11*, 35.
[47] J. N. Israelachvili, *Intermolecular and Surface Forces*, Academic Press, Oxford, UK **2011**.
[48] J. Hesselbach, J. Wrege, A. Raatz, *Ann. CIRP* **2007**, *56*, 45.
[49] S. Van Aert, K. J. Batenburg, M. D. Rossell, R. Erni, G. Van Tendeloo, *Nature* **2011**, *470*, 374.
[50] B. Goris, S. Bals, W. Van den Broek, E. Carbó-Argibay, S. Gómez-Graña, L. M. Liz-Marzán, G. Van Tendeloo, *Nat. Mater.* **2012**, *11*, 930.
[51] M. C. Scott, C.-C. Chen, M. Mecklenburg, C. Zhu, R. Xu, P. Ercius, U. Dahmen, B. C. Regan, J. Miao, *Nature* **2012**, *483*, 444.
[52] W. J. Huang, J. M. Zuo, B. Jiang, K. W. Kwon, M. Shim, *Nat. Phys.* **2009**, *5*, 129.
[53] C. L. Jia, S. B. Mi, J. Barthel, D. W. Wang, R. E. Dunin-Borkowski, K. W. Urban, A. Thust, *Nat. Mater.* **2014**, *13*, 1044.
[54] J. Park, H. Elmlund, P. Ercius, J. M. Yuk, D. T. Limmer, Q. Chen, K. Kim, S. H. Han, D. A. Weitz, A. Zettl, A. P. Alivisatos, *Science* **2015**, *349*, 290.
[55] I. N. Tang, K. H. Fung, in *Proc. 1988 Sci. Conf. on Obscuration and Aerosol Research*, US Army Chemical Research, Development & Engineering Center (CRDEC), Aberdeen Proving Ground, MD, USA **1989**, p. 355.
[56] S. A. Blanton, A. Dehestani, P. C. Lin, P. Guyot-Sionnest, *Chem. Phys. Lett.* **1994**, *229*, 317.

© 2017 WILEY-VCH Verlag GmbH & Co. KGaA, Weinheim